Stress and seismicity related to cooling of geothermal wells

Arno Zang[1,2], Hannes Hofmann[1,3], Gergő András Hutka[1,3], Bakul Mathur[1], Mauro Cacace[1]
[1]*Helmholtz Centre Potsdam GFZ German Research Centre for Geosciences, Potsdam, Germany*
[2]*Institute of Geosciences, University of Potsdam, Germany*
[3]*Institute for Applied Geosciences, Technical University of Berlin, Germany*

Serge Shapiro[4]
[4]*Institute of Geosciences, Free University of Berlin, Germany*

Beau Whitney[5], Cedric Duvail[5], Ramon Secanell Gallart[5]
[5]*Fugro NL Land BV, Groningen, The Netherlands*

Niels Grobbe[6], Annemarie Muntendam-Bos[6]
[6]*Dutch State Supervision of Mines, The Hague, The Netherlands*

ABSTRACT: Deep geothermal energy (~3-6 km depth) is a candidate for sustainable and carbon-free energy supply. One of the main concerns of deep geothermal systems is induced seismicity that may produce earthquakes of economic concerns, challenging the development of this form of alternative energy. So far, cold water injection has been overlooked but may contribute to induced seismicity due to fault reactivation through thermal stresses also beyond the cooling region. This can be of importance, in particular, in fractured and faulted geothermal reservoirs. In this study, we first compare different approaches to estimate induced seismic risk from slip-tendency analysis, rate-and-state friction theory and modified Gutenberg-Richter statistics based on frictional Coulomb-stress perturbations. Then, we systematically investigate effects of both, intrinsic geological parameters (e.g., fault-, host rock properties and in-situ stress), and operational parameters (e.g., well geometry and placement, injection schemes, induced pressure perturbation) on induced seismicity.

Keywords: Coulomb failure stress, deep geothermal energy, induced seismicity, rate-and-state friction theory and thermo-hydraulic-mechanical modelling.

1 INTRODUCTION AND SCOPE

One of today's greatest challenges is the energy transition from fossil fuels to low-carbon renewables. Geothermal energy is a local solution for base load heat and electricity supply. As such it has the potential to provide safe and clean energy for the growing urban areas worldwide. In the Netherlands, geothermal energy is conventionally extracted from deep sedimentary aquifers that may be intersected by fractures and faults. While fault zones may serve as fluid pathways, thereby improving fluid production from and injection to a reservoir, they also pose the risk of hosting seismic events caused by geothermal operations (Muntendam-Bos et al. 2022, Buijze et al. 2020, Zang et al. 2014). The risk of induced seismicity is a major factor that currently hinders the widespread development of geothermal energy. Injection-induced seismic risk must thus be better understood to develop methods to assess and mitigate the risk of larger induced seismic events (Bommer 2022).

Injection of fluid in the subsurface can cause overpressure that reduces the effective stress and causes induced seismicity (Ellsworth 2013). Injection of cold water into a hot reservoir induces thermal stresses due to rock mass contraction (De Simone et al. 2013, Kivi et al. 2022) and is another cause of induced events. If the stress state is isotropic, fracture activation is dominated by late-stage thermal drawdown; if the stress state is anisotropic (stress deviator), fractures are critically stressed and small pressure increase can reactivate fractures multiple times (Jing et al. 2022). Based on a showcase from the Californie site, Vörös and Baisch (2022) suggested to relocate one of the injection

wells further away from the Tegelen fault in the Roer Valley rift system to mitigate the risk of induced events.

In the Netherlands, geothermal energy is commonly utilized by producing hot fluid from a sedimentary reservoir through a producer, extracting the heat at the surface via a heat exchanger, and re-injecting the cold fluid via an injector (well doublet). This re-injection operation cools down the reservoir, which triggers a variety of coupled thermo-hydro-mechanical processes leading to changes in the effective normal stress and shear stress acting on a fault. Given that the Dutch subsurface is commonly intersected by normal faults, these stress changes induced by existing and planned geothermal systems may then result in sudden slip of nearby faults, which could potentially be associated with seismic release of the stored energy. It is therefore required to improve the understanding of the thermo-hydro-mechanical effects due to cold water injection in geothermal systems. Of particular interest is the influence of operational parameters such as injection temperature, injection pressure/rate, injected volume and distance to faults, and the influence of geological boundary conditions such as rock properties, fault properties and the in-situ and dynamic stress field on induced seismicity. This will allow to develop better guidelines and tools for safe exploration, development and operation of geothermal systems.

In this paper, based on a review of processes governing induced seismicity, and a review of the geology of the Netherlands, we first setup generic and specific modelling scenarios. Second, we used three different modelling approaches to assess induced seismic hazard: slip tendency analysis, rate-and-state friction theory and a Coulomb stress change model. The slip tendency (Blöcher et al., 2018) and Coulomb stress change models (Cacace et al., 2021) were verified by history matching injection operations at the Groß Schönebeck Enhanced Geothermal System (EGS) site. The rate-and-state friction model was verified by history matching laboratory tests (Hutka et al., 2023). A translation of the Coulomb stress change model results in site-specific seismic intensities.

2 MODEL SETUP AND METHODS

The two typically exploited geothermal reservoir formations, as well as a likely target for EGS, in the Netherlands are the Slochteren Sandstone, the Delft Sandstone and the Dinantian Limestone, respectively. We choose these formations as the basis for our modelling studies. While the Delft and Slochteren Sandstone reservoirs represent matrix-dominated systems with high porosity and permeability, the Dinantian Limestone represents a fracture-dominated system which may be exploited by drilling into fault zones or developing EGS. Modelling scenarios consider a geothermal well doublet with respect to a fault zone in target rock formations like Slochteren Sandstone, Delft Sandstone and Dinantian Limestone typical for the subsurface in The Netherlands. Also, a multi-stage EGS approaching a fault zone is modelled in the Dinantian Limestone. All numerical modelling studies were performed with the flexible parallel implicit finite element code GOLEM, which is based on the Multiphysics modelling framework MOOSE (Jacquey and Cacace 2017). While using the same underlying coupled thermo-hydro-mechanical processes (Mathur et al., 2021), three complementary approaches were used to assess the induced seismic hazard: slip tendency analysis, rate-and-state friction theory and Coulomb failure stress changes (Table 1). In the slip tendency analysis (Table 1, first row), a base case model for the Slochteren formation (Rotliegend) was simulated, a sensitivity analysis of the most important model parameters was carried out, and specific models of the Slochteren, Delft and Dinantian formations were investigated. The model was calibrated in a previous study on the EGS site Groß Schönebeck, where a slip tendency analysis for long-term cold-water injection was performed in a Rotliegend reservoir in the North German Basin (Blöcher et al., 2018).

The rate-and-state friction model (Table 1, mid row) was implemented in GOLEM in the frame of this project, and a laboratory fault activation experiment was used for model calibration and analysis of the fault slip behavior (Hutka et al., in press). The modelling approach, calibration results and fault slip analysis are provided in detail in Hutka et al. (2023). The field scale rate-and-state friction model was not used in the generic modelling study (sensitivity analysis), but only for the specific base case Slochteren model (Mathur et al. NJG submitted). The theory of the Coulomb failure stress (CFS) change model used in this study (Table 1, right column) was also developed in

the framework of this project. The theory has been implemented in GOLEM and validated against the Groß Schönebeck field case (Cacace et al. 2022). The CFS model was used in the generic modelling scenarios (sensitivity analysis for Slochteren Sandstone) and in the specific modelling scenarios (Slochteren, Delft, Dinantian). The results of the base case Slochteren Sandstone CFS model were used as input for the seismic intensity calculations.

Table 1. Approaches to assess fault slip and induced seismic hazard.

Model	**Theory***	**Validation**	**Output**	**Benefits**
Slip tendency analysis (ST); Mathur et al.	$\mathrm{ST} = \frac{\lVert\tau\rVert}{\lVert\sigma_N - p\rVert} \geq \mu$	Groß Schönebeck (*Blöcher et al., 2018*)	Slip tendency on fault patches	State-of-the-art fault stability assessment for known faults
Rate and state friction (RSF); Dieterich (1979) Dieterich (1981), Ruina (1983)	$\tau + \delta\tau_{qs} - \beta_{rad}V = \mu\left(\sigma_N - p + \delta\sigma_{qs}\right)$ $\tau(t) = a\,\sigma_N(t)\cdot \mathrm{arcsinh}\left[\frac{V(t)}{2V_0}\exp\left(\frac{\theta(t)}{a}\right)\right]$ $\frac{\partial\theta(t)}{\partial t} = -\frac{V(t)}{D_c}(\mu - \mu_{ss})$ $\mu_{ss} = \mu_0 + (a-b)\cdot \ln(V(t)/V_0)$ $M_0 = \int G\,u\,dA$	Laboratory slip experiment (*Hutka et al., 2023*)	Fault slip velocities	Friction dynamics is taken into account
Coulomb failure stress (δCFS); Shapiro et al (2010), Shapiro (2018)	$\delta CFS = \delta\tau - \mu(\delta\sigma_N - \delta p)$ $\log_{10}[N_{\geq M}(t)] = [\Sigma_0 + \delta\Sigma(t)] - bM$ $\delta\Sigma(t) = \log_{10}[\int_V \frac{S\,M[\delta CFS(\mathbf{x},t)]}{\sin(\varphi)}dV]$ $N_{\geq M}(t) = 10^{(\Sigma_0 - bM)}\int_V \frac{S\,M[\delta CFS(\mathbf{x},t)]}{\sin(\varphi)}dV$ $< M_{max}(t) >= \frac{1}{b}(\Sigma_0 + \log_{10}[\int_V \frac{S\,M[\delta CFS(\mathbf{x},t)]}{\sin(\varphi)}dV])$	Groß Schönebeck (*Cacace et al., 2021*)	Seismic catalogue considering the whole reservoir volume	Considers unknown faults in the seismic hazard assessment

*) Compressive stress is assumed to be positive. ST: slip tendency, τ: shear stress, σ_N: normal stress, *p:* fluid pressure, μ: friction coefficient, $\delta\tau_{qs}$: quasi-static shear stress, β_{rad}: radiation damping coefficient, V: slip velocity, $\delta\sigma_{qs}$: quasi-static normal stress, a: scalar expressing direct frictional change, V_0: reference slip velocity, θ: state variable, D_c: critical slip distance, b: scalar expressing frictional change over D_c, μ_{ss}: static friction coefficient at $V = 0$, μ_0: nominal friction coefficient at $V = V_0$, M_0: seismic moment, G: shear modulus, u: shear displacement, dA: fault area, δCFS: variation of Coulomb failure stress, $\delta\tau$: variation of shear stress, $\delta\sigma_N$: variation of normal stress, δp: variation of fluid pressure, $N_{\geq M}$: number of seismic events with magnitudes larger than M, Σ_0: seismogenic index, S: uniaxial storage coefficient, M[δ CFS]: minimum positive monotonic majorant of δ CFS, φ: friction angle, $< M_{max} >$: expected maximum magnitude.

All reservoir models were setup in a similar fashion. The coordinates of the model were aligned with the maximum and minimum horizontal stress directions. The mesh was created with MeshIt (Cacace et al. 2015). Mesh refinement was applied around the wellbores, on the fault and inside the reservoir unit (Fig. 1c). A steady state simulation was performed first to initialize the model followed by a 30 years transient simulation with cold water injection and production with the same flow rate.

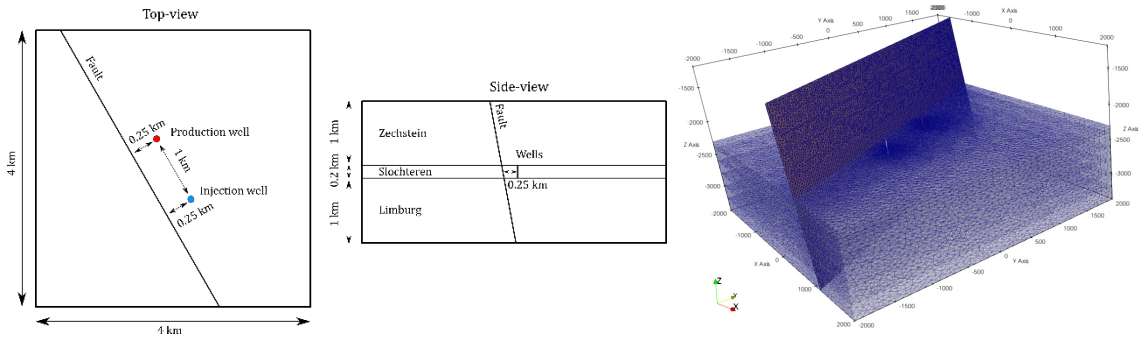

Figure 1. Base case model with well doublet, fault and three rock layers. (a) Top view, (b) side view geometry, and (c) snapshot of 3D finite element mesh. Unit top is 2000 m, 2200 m and 2400 for Zechstein, Rotliegend and Limburg with 200 m thickness. Fault strike is N130°E, dip is 80° from horizontal and NE.

Table 2. Properties of geological units and the fault in the base case model.

Model property	**Zechstein (rock salt)**	**Rotliegend (sandstone)**	**Limburg (claystone)**
Young's modulus (GPa)	30	15 (3-30)	40
Poisson's ratio (-)	0.3	0.2 (0.1-0.25)	0.2
Solid bulk modulus (GPa)	30	59.5	50
Drained bulk modulus* (GPa)	25	8.33 (1.3-20)	22.2
Biot coefficient* (-)	0.17	0.86 (0.5-0.97)	0.56
Solid thermal conductivity (W/m/°C)	4.5	3.5	2.0
Solid heat capacity (J/kg/°C)	925	830	860
Volumetric bulk thermal expansion coefficient (1e-6/°C)	30	30	30
Solid density (kg/m³)	2170	2650	2650
Hor. permeability (mD)	0.001	100	0.001
Hor./vert. permeability (-)	1	2	1
Porosity (%)	1	20	1

2.1 Slochteren Base Case Model

The Slochteren sandstone model is simplified to three horizontal geological units: Zechstein (top), Slochteren (reservoir in the middle) and Limburg (bottom), Fig. 1b. All three three-dimensional units are intersected by a two-dimensional fault indicated as line (Fig. 1ab) and planar discontinuity (Fig. 1c, vertical plane). Two vertical one-dimensional lines represent the injection and production well (Fig. 1ab, blue and red dot), which intersect the entire reservoir unit (Fig. 1b, vertical line). Figure 1 illustrates the top view (a), side view of the Slochteren base case model (b), and a snapshot of the base case model 3D mesh (c). Mechanical, hydraulic and thermal properties of the rock matrix of reservoir, top and bottom unit as well as fault properties can be found in Table 2 together with fluid properties. The summary of the base case model boundary and initial condition is as follows: temperature gradient 31°C/km + 10°C, pore pressure gradient (11 MPa/km), stress gradient (23, 15, 14 MPa/km for SV, SH, Sh) with SH-direction N160°E; fluid density 1154 kg/m^3, initial fluid viscosity 0.68 mPas, fluid specific heat capacity 3240 J/kg/°C, fluid bulk modulus 3.4 GPa and seismogenic index -4.5.

2.2 Dinantian Multi-stage EGS Model

The Dinantian carbonate formation is the deepest formation we consider in this analysis. Here, we simplify the geology to a horizontal Limburg claystone layer as top seal, a horizontal Dinantian limestone layer as reservoir layer and a horizontal Devonian claystone-sandstone layer as bottom seal. Due to the low permeability of the rock matrix we consider three models for geothermal exploitation of the Dinantian limestone: (a) wells intersect a high permeability fault, (b) wells intersect a fault zone with damage zone, and (c) hydraulically fractured parallel horizontal wells are drilled next to the fault representing a multi-stage EGS model.

3 RESULTS

3.1 Slochteren base case model results

With the base case model geometry and parameters, the model showed a potential fault failure after 11 years of cold-water injection when the maximum slip tendency on the fault reaches the critical value of 0.6. Figure 2 shows the pressure and temperature contours around the injection well and the slip tendency on the fault plane after 29 years of circulation. The slip tendency values are increasing when the cold thermal front reaches the fault plane (Fig. 2, left). The pressure perturbation due to the injection process on the other hand, quickly stabilizes and does not produce discernible changes in the slip tendency on the fault plane (Fig. 2, fast-dropping sugar-cone shaped pressure contours close to vertical well). The figure shows increased thermal stresses at the formation intersections (Fig. 2, far-reaching balloon-shaped temperature contours from vertical well). This occurs due to the higher rock stiffness of the top and the bottom layers, as the magnitude of the thermal stress depends linearly on the Young's modulus. That is, a higher Young's modulus leads to a higher induced seismic hazard potential (Segall & Fitzgerald, 1998). The maximum pore pressure increase around the injection well is ~3.8 MPa. The temperature around the injection well reaches the injection water temperature i.e. 30°C. Cooling will cause shrinkage of rock, and mismatch of mineral moduli will support cracking processes. Fractured host rock close to the fault will allow slip more easily. The combined effect of the thermal, hydraulic and mechanical processes result in an overall increased slip tendency on the fault. After 30 years of cold water injection about 0.077 km^2 fault area undergoes failure. The maximum slip tendency of the fault plane is 0.85 within the reservoir.

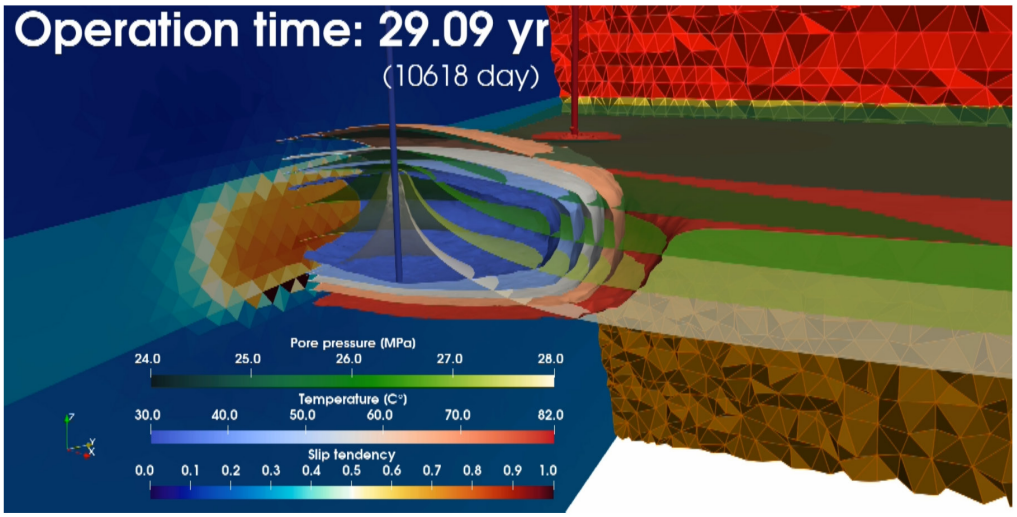

Figure 2. Base case model results: Pore pressure (sugar-cone shaped contours close to) and temperature (balloon shaped contours further away from) the injection well (blue vertical line), and slip tendency projected onto the fault (left) after 29 years of fluid circulation.

To understand the impact of the most important reservoir geometries, geological and operational parameter, a sensitivity analysis was performed within the base case model. The five parameters that constitute the thermal and mechanical governing equations have the highest impact on the fault failure potential: (1) the minimum horizontal stress gradient; (2) geo-mechanical reservoir properties like Young's modulus and Poisson's ratio; (3) distance between the wells and the fault; (4) re-injection temperature and flow rate, and (5) other geological properties like temperature and pressure gradients, thermal expansion coefficient, fault dip, reservoir depth and porosity of the reservoir rock.

Many of these parameters also impact the magnitudes of maximum temperature change on the fault. This indicates a strong correlation between the thermal stresses and slip tendencies. However, such correlation was not observed with the maximum change in pressure values. Parameters such as pore-pressure differential, permeability, fluid viscosity did not impact the slip tendency of the fault, indicating that the hydraulic governing equation did not play a significant role in the fault failure mechanism. The cases with higher slip tendencies also resulted in a larger area of the fault with a potential to fail. These cases also failed earlier than the cases with low slip tendency values.

3.2 Dinantian multi-stage EGS model results

As compared to the fault-dominated exploitation of the Dinantian limestone reservoir, the EGS models shows significantly lower potential of fault failure. The injection water in the EGS models is distributed into the reservoir unit through the hydraulic fractures. Especially the temperature changes are thus confined to the near wellbore areas around the injection well, thus having a low impact on the stress changes on the fault plane. Figure 3 shows the slip tendency on the fault plane in the EGS models after 30 years of circulation. The EGS system with 500 m distance between the injection well and the fault shows no failure potential whereas the EGS model with 250 m distance between the injection well and the fault shows failure potential after 28.7 years.

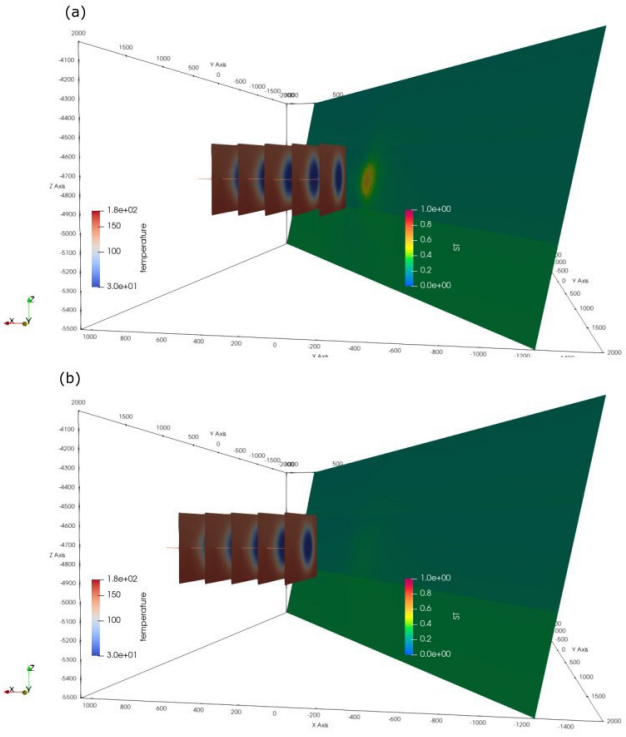

Figure 3. Comparison of temperature distribution on hydraulic fractures (five square patches to the left) and slip tendency on the fault (large rectangular area to the right) after 30 years of fluid circulation in the Dinantian multi-stage EGS model with (a) 250 m well-fault spacing, and (b) 500 m fault-well spacing.

4 DISCUSSION

The 3D finite element study suggests that the changes in the slip tendency of a planar 2D fault discontinuity without cohesion can largely be attributed to thermo-mechanical effects. While the direct pore pressure effect on the slip tendency does not change after a new equilibrium is reached in a doublet system after a couple of months, the cold-water front continues to grow around the injection well as long as the injection well is in operation. A significant increase in the slip tendency was observed when this low temperature front reached the fault zone. Besides the obvious importance of the stress field and the local fault geometry, rock mechanical properties and operating conditions have a major influence on the induced stress changes and the related fault activation potential triggered by geothermal operations. Thus, careful selection of a suitable target formation and the operational parameters is crucial to minimize the risk of induced seismicity. Lower regional stress, temperature and pressure gradients, lower reservoir rock stiffness, shallower depth, higher reservoir porosity, larger reservoir thickness, lower thermal expansion coefficient and higher fault dip contribute to a lower risk geothermal environment. Besides selecting a low risk geothermal formation, the failure potential can further be minimized by optimizing operational factors. The key planning and operational parameters to be considered include the respect distance between the fluid-injection well and existing known faults, re-injection temperature and injection flow rate. During the geothermal operations, the most effective measures to reduce the risk of induced seismicity are increasing the re-injection temperature and decreasing the injection rate. The EGS system with optimized well-to-fault spacing can be an effective technique for the mitigation of induced seismicity in deeper reservoirs such as Dinantian limestone. Even though the slip tendency may indicate fault failure, it does not give hints about how the energy and the seismicity is expected to be released from this fault failure. By applying a rate and state friction framework to the same model with friction parameters measured in the laboratory on Dutch Rotliegend faults, we find that the modelled fault slip is likely to be aseismic.

A limitation of the current model is the lack of validation with the field observations. No induced seismicity has been monitored in the conventional matrix-type geothermal reservoirs in the Netherlands, whereas previously observed induced seismicity in a Dinantian limestone reservoir at Californie site indicates the need of a detailed analysis of the geological and operational settings of EGS systems (Vörös and Baisch 2022). In this study, we carried out a generalized sensitivity analysis with simplified models. Potential future studies can include site specific model geometries, further refined meshes, a non-linear failure criterion, poroelastic coupling and a creep constitutive law for the Zechstein salt. It has to be noted that implementing more realistic fault systems (e.g., en echelon and segmented faults) will have a major impact on the results presented in this study.

5 CONCLUSIONS

Our results of Dutch geothermal well doublet thermo-hydro-mechanical models indicate that thermal effects play a major role in fault stability. Cooling induced thermal stresses are tensile in nature, thereby reducing the magnitude of the resulting compressive stresses. This increases the slip tendency of the fault. Thermal stresses are highly sensitive to geo-mechanical reservoir rock properties. The higher the rock stiffness, the higher the chances of failure during cold fluid injection. For Slochteren sandstone, a stable fault configuration has a higher fault dip and fault strike at higher angle with maximum stress direction for the range of investigated geometries. The sensitivity analysis suggests that a greater difference in stress gradients in different principal directions leads to high shear stresses. This results into higher failure potential of the fault. Among the thermal properties, bulk thermal expansion coefficient has the most significant effect on fault stability. Well-to-fault distance, re-injection temperature, and injection flow rate are key parameters that can influence the seismic risk.

ACKNOWLEDGEMENTS

This project has been funded by the “Kennis Effecten Mijnbouw” (KEM)-programme through the project “Risk of seismicity due to cooling effects in geothermal systems – KEM-15”. H.H. and G.A.H. kindly acknowledge the financial support of the Helmholtz Association’s Initiative and Networking Fund for the Helmholtz Young

Investigator Group ARES. N.G., A.G.M.-B, and Richard Bakker (R.B. is no longer with SodM) conceptualized the study, provided guidance, and contributed to discussions that further improved the results. As sponsor, SodM retains the right to carry out its own final assessment of the impact of the outcomes of the study.

REFERENCES

Blöcher G., Cacace M., Jacquey A.B., Zang A., Heidbach O., Hofmann H., Kluge C., Zimmermann G. 2018. Evaluating Micro-Seismic Events Triggered by Reservoir Operations at the Geothermal Site of Groß Schönebeck (Germany). Rock Mechanics and Rock Engineering 51 (10), 3265-3279.

Bommer J.J. 2022. Earthquake hazard and risk analysis for natural and induced seismicity: towards objective assessments in the face of uncertainty. Bulletin of Earthquake Engineering 20, 2825–3069.

Buijze L., Lonneke v. B., Cremer H., Paap B., Veldkamp H., Wassing B. T., Wees J. D., Yperen G. C. N., Jaarsma B., Heege J. H. 2020. Review of induced seismicity in geothermal systems worldwide and implications for geothermal systems in the Netherlands. Netherlands Journal of Geosciences 99, e10.

Cacace M. & Blöcher G. 2015. MeshIt - a software for three dimensional volumetric meshing of complex faulted reservoirs. Environmental Earth Sciences 74, 5191-5209.

Cacace, M., Hofmann H., Shapiro, S. 2022. Projecting seismicity induced by complex alterations of underground stresses with applications to geothermal systems. Scientific Reports 11, 23560. https://doi.org/ 10.1038/s41598-021-02857-0

De Simone S, Vilarrasa V, Carrera J, Alcolea A, Meier P (2013) Thermal coupling may control mechanical stability of geothermal reservoirs during cold water injection. Phys. Chem. of the Earth 64, 117-126

Dieterich, J. H. 1979. Modelling of rock friction: 1. Experimental results and constitutive equations. Journal of Geophysical Research: Solid Earth 84, 2161–2168.

Dieterich, J. H. 1981. Constitutive properties of faults with simulated gouge. Mechanical Behavior of Crustal Rocks 24, 103–120.

Ellsworth, W.L. 2013. Injection-induced earthquakes. Science https://doi.org/10. 1126/science.1225942

Hutka, G. A., Cacace, M., Hofmann, H., Zang, A., Wang, L., & Ji, Y. 2023. Numerical investigation of the effect of fluid pressurization rate on laboratory-scale injection-induced fault slip. Scientific Reports, 13(1), 4437.

Hutka G.A., Cacace M., Hofmann H., Mathur B., and Zang A. 2023. Investigating seismicity rates with Coulomb failure stress models caused by pore pressure and thermal stress from operating a well doublet in a generic geothermal reservoir in the Netherlands. Netherlands Journal of Geosciences, Volume 102, e8. https://doi.org/ 10.1017/njg.2023.7

Jacquey, A.B. & Cacace, M. 2017. GOLEM, a MOOSE-based application. https://doi.org/10.5281/zenodo.99940

Kivi I.R., Pujades E., Rutqvist J., Vilarrasa V. 2022. Cooling-induced reactivation of distant faults during long-term geothermal energy production in hot sedimentary aquifers. Scientific Reports 22, 2065.

Mathur B., Hofmann H., Cacace M., Hutka G., Zang A. (under review). Thermo-hydro-mechanical simulation of cooling-induced fault reactivation in Dutch geothermal reservoirs. Netherlands Journal of Geosciences.

Muntendam-Bos A.G., Hoedeman G., Polychronopoulou K., Draganov D., Weemstra C., van der Zee W., Bakker R.R., and Roest H. 2022. An overview of induced seismicity in the Netherlands. Netherlands Journal of Geosciences, Volume 101, e1. https://doi.org/10.1017/njg.2021.14

Ruina, A. 1983. Slip instability and state variable friction laws. Journal of Geophysical Research: Solid Earth 88, 10359–10370.

Segall, P. & Fitzgerald, S.D., 1998. A note on induced stress changes in hydrocarbon and geothermal reservoirs. Tectonophysics 289(1–3): 117–128.

Shapiro, S. A., Dinske, C., Langenbruch, C., & Wenzel, F. 2010. Seismogenic index and magnitude probability of earthquakes induced during reservoir fluid stimulations. The Leading Edge, 29(3), 304-309.

Shapiro, S. A. 2018. Seismogenic index of underground fluid injections and productions. Journal of Geophysical Research: Solid Earth, 123(9), 7983-7997.

Vörös R., Baisch S. 2022. Induced seismicity and seismic risk management – a showcase from Californie geothermal field (the Netherlands). Netherland Journal of Geosciences 101, e15.

Zang A., Oye V., Jousset P., Deichmann N., Gritto R., McGarr A., Majer E., Bruhn D. 2014. Analysis of induced seismicity in geothermal reservoirs – An overview. - Geothermics 52, 6-21.